Development 136, 2403-2411 (2009) doi:10.1242/dev.035410

Cell rearrangements, cell divisions and cell death in a migrating epithelial sheet in the abdomen of *Drosophila*

Marcus Bischoff[1,2,*] and Zoltán Cseresnyés[1]

During morphogenesis, cell movements, cell divisions and cell death work together to form complex patterns and to shape organs. These events are the outcome of decisions made by many individual cells, but how these decisions are controlled and coordinated is elusive. The adult abdominal epidermis of *Drosophila* is formed during metamorphosis by divisions and extensive cell migrations of the diploid histoblasts, which replace the polyploid larval cells. Using in vivo 4D microscopy, we have studied the behaviour of the histoblasts and analysed in detail how they reach their final position and to what extent they rearrange during their spreading. Tracking individual cells, we show that the cells migrate in two phases that differ in speed, direction and amount of cellular rearrangement. Cells of the anterior (A) and posterior (P) compartments differ in their behaviour. Cells near the A/P border are more likely to change their neighbours during migration. The mitoses do not show any preferential orientation. After mitosis, the sisters become preferentially aligned with the direction of movement. Thus, in the abdomen, it is the extensive cell migrations that appear to contribute most to morphogenesis. This contrasts with other developing epithelia, such as the wing imaginal disc and the embryonic germband in *Drosophila*, where oriented mitoses and local cell rearrangements appear to direct morphogenesis. Furthermore, our results suggest that an active force created by the histoblasts contributes to the formation of the adult epidermis. Finally, we show that histoblasts occasionally undergo apoptosis.

KEY WORDS: Morphogenesis, Cell migration, Cell division orientation

INTRODUCTION

How do groups of cells form complex patterns during morphogenesis? Cell movements, cell divisions and cell death work together to place cells in their final positions. Notable examples are provided by cell movements in early nematode development (Schnabel et al., 2006), dorsal closure (Jacinto et al., 2000) and gastrulation movements in *Drosophila* (McMahon et al., 2008), as well as convergent extension movements (Keller, 2002) and primitive streak formation (Voiculescu et al., 2007) in vertebrate development. Even though the cells move together as groups (Lecaudey and Gilmour, 2006), it is the behaviour of the individual cells that directs morphogenesis. Although new imaging techniques have recently lead to progress in the analysis of patterning (Keller et al., 2008), the mechanisms underlying the final positioning of cells remain elusive.

Oriented mitoses are thought to play some role in *Drosophila* wing development (Baena-Lopez et al., 2005) and germband extension (da Silva and Vincent, 2007) as well as in zebrafish gastrulation (Gong et al., 2004) and neurulation (Tawk et al., 2007). However, during morphogenesis, cells often divide and migrate at the same time. Thus, it becomes difficult to separate the contributions of mitosis and cell movement to morphogenesis, and for this reason the specific contribution of oriented mitosis to patterning remains unclear (da Silva and Vincent, 2007; Gong et al., 2004).

In some developmental contexts, the removal of cells by apoptosis is important for patterning, e.g. in leg imaginal disc development in *Drosophila* (Manjon et al., 2007) and limb development in vertebrates (Chen and Zhao, 1998).

[1]Department of Zoology, University of Cambridge, Downing Street, Cambridge CB2 3EJ, UK. [2]MRC Laboratory of Molecular Biology, Hills Road, Cambridge CB2 0QH, UK.

*Author for correspondence (e-mail: mb628@cam.ac.uk)

Accepted 19 May 2009

In epithelia, adherens junctions ensure the integrity of the tissue and give it some rigidity. Consequently, cell rearrangements during epithelial morphogenesis are limited and depend on the remodelling of cell-cell junctions (Bertet et al., 2004). Examples are the wing imaginal disc and the elongation of the embryonic germband of *Drosophila*, where oriented mitoses and local cell rearrangements (with only limited changes in neighbourhood relations) drive morphogenesis (Baena-Lopez et al., 2005; da Silva and Vincent, 2007; Blankenship et al., 2006; Classen et al., 2005; Gibson et al., 2006; Irvine and Wieschaus, 1994).

The adult epidermis of the abdomen of *Drosophila* is newly formed during metamorphosis as the polyploid larval epithelial cells (LECs) are replaced by the descendants of the histoblasts –diploid imaginal cells derived from small lateral nests in the larva. The histoblasts divide and migrate dorsally and ventrally over the abdomen until its whole surface is covered with cells (Madhavan and Madhavan, 1980; Ninov et al., 2007; Roseland and Schneiderman, 1979). During this process, the LECs undergo apoptosis; they constrict apically, are extruded from the epithelium and are subsequently phagocytosed by hemocytes, which patrol underneath the epithelium (Ninov et al., 2007).

We have tracked individual cells using 4D microscopy (Schnabel et al., 1997) in order to study the morphogenesis of the adult abdominal epidermis of *Drosophila* in detail. We have investigated which cellular behaviours are important to this process and to what extent cells rearrange during the spreading of the histoblasts. We show here that there are two phases of cell migration. In the anterior (A) and posterior (P) compartments, cells differ in their behaviour. The A/P boundary appears to influence the behaviour of cells near to it. In contrast to in other epithelia (Baena-Lopez et al., 2005; da Silva and Vincent, 2007), we find that cell migrations dominate patterning in the abdominal epidermis; the mitoses do not show any preferential orientation, but following mitosis the two sisters become preferentially aligned with the direction of movement. Our results furthermore suggest that the migrating histoblasts might actively contribute to

their own movement, thus pushing against the larval cells. Finally, we observe that histoblasts occasionally die and are removed from the epithelium.

MATERIALS AND METHODS

Fly stocks and clonal analysis

FlyBase (Grumbling and Strelets, 2006) entries of the mutations and transgenes are as follows: *en.Gal4*, *Scer/Gal4$^{en\text{-}e16E}$*; *tub.Gal80*, *Scer\Gal80$^{alphaTub84B.PL}$*; *tub.Gal4*, *Scer\Gal4$^{alphaTub84B.PL}$*; *UAS.RedStinger*, *Disc\RFP$^{DsRedT4.Scer\UAS.T:nls5}$*; *H2AvGFP*, *His2Av$^{T:Avic\GFP\text{-}S65T}$* (Clarkson and Saint, 1999); *Sqh::GFP*, *sqh$^{T:Avic\GFP}$* (Royou et al., 2002); and *DE-cadherin::GFP*, *shg$^{Ubi\text{-}p63E.T:Avic\GFP\text{-}rs}$* (Oda and Tsukita, 2001).

Pupae carrying 'wild-type' clones marked with DsRed had the following genotype: *y w hs.FLP; H2AvGFP/+; tub<Gal80<Gal4/UAS.RedStinger*.

Overexpression clones were induced using the FLP-out technique (Struhl and Basler, 1993). Clones were induced by heat shocking third instar larvae for 1 hour at 35°C.

4D microscopy

For imaging, pupae were staged according to Bainbridge and Bownes (Bainbridge and Bownes, 1981). A window in the pupal case was made and the pupae were filmed as described (Escudero et al., 2007). All the studied flies developed into pharate adults after imaging and many eclosed. *z*-stacks of ~40 μm with a step size of 2.5 or 3.0 μm were recorded every 120, 150 or 180 seconds using a Biorad MRC-1024 or a Leica SP5 confocal microscope at 23-25°C.

We focused our analysis on segment 2 because it is not anatomically distinct from other segments (such as segment 1) and it is the easiest to image owing to the roundish shape of the abdomen. We followed cells at the tip of the dorsally moving cell mass in the last ~15 hours prior to arrival of the histoblasts at the dorsal midline. To track the cells, we marked them with a nuclear Histone::GFP marker (Clarkson and Saint, 1999). In some pupae, we also expressed nuclear DsRed using an *en.Gal4* driver to mark cells of the P compartments. The selector gene *engrailed* (*en*) is expressed in stripes of all P compartment cells in the abdomen (Struhl et al., 1997).

The cylindrical shape of a pupa does not allow filming of the dorsal histoblast nests and the dorsal midline at the same time. To film the entire movement of the cells of the dorsal histoblast nests, some pupae were rolled under the microscope during the recording by moving the coverslip using a screw-operated pushing mechanism in a custom-made metal chamber (Fig. 1A,B; see Movie 1 in the supplementary material; *n*=5 pupae).

The movies were exported from the confocal software as image sequences comprising single TIF files and analysed using SIMI Biocell (Schnabel et al., 1997) (www.simi.com). For presentation, the image sequences were maximum projected using ImageJ (NIH, Bethesda). The figures and movies were prepared using Adobe Illustrator, Adobe Image Ready, Adobe Photoshop, ImageJ, Volocity (Improvision) and Quicktime Pro (Apple).

Analysis of 4D movies

In the 4D movies, the cells were tracked manually using SIMI Biocell. The 3D coordinates of the nuclei were saved at least every 30 minutes as well as 1 frame before and 1, 2, 5, 10, 20 and 30 frames after mitosis. Furthermore, the times of all divisions were stored, thus building the lineages of all tracked cells. The 3D representations and the paths the cells followed were generated with SIMI Biocell. We used fluorescent Histone markers, which are well-suited to follow cell divisions because the metaphase plate and the anaphase chromosomes can be seen; the time interval between the *z*-stacks allowed us to observe both structures, thus enabling a proper evaluation of cell divisions.

The following parameters were calculated using a program written in C# using Microsoft Visual Studio 2005 with the Microsoft.NET 2.0 framework. All calculations were performed in two dimensions owing to the planar character of the epithelial sheet (see Fig. S1 in the supplementary material).

Cell division orientation

To calculate the angle of cell division (∂), we used the 2D coordinates of the sister cells during anaphase (one frame after the metaphase plate is visible). The angle was calculated between the line connecting these points and the dorsoventral (DV) axis of the pupa.

Sister cell rearrangement

To calculate the position of sister cells relative to each other (ρ), we used the last 2D coordinate of the lineage of the two sisters (either before the next mitosis or at the end of the movie) and calculated the angle between the line connecting these points and the DV axis of the pupa. The average time between mitosis and the last coordinate of a cell is 162±90 frames (~7±4 hours).

Cell density

To calculate the density maps, the distance of each cell to its six nearest neighbours was calculated at a given time point and the average distance plotted at the position of the cell using a 16-band look-up table (LUT). This algorithm introduces an error at the borders of the cell mass because these cells have fewer neighbours on one side.

Neighbourhood maps

To calculate the neighbourhood maps, we used the 2D coordinates of all cells at two given time points (the start and the end of the movie). For each cell, the distances to the six closest neighbours at time point 1 were calculated. Then, the distances to the same six cells (regardless of whether they remained closest neighbours or not) were calculated at time point 2. For each of the six neighbours, the difference between these two values was calculated and then the average was plotted at the position of the cell at time point 1 using a banded LUT. Since this calculation is affected by the observed change in cell density over time (cells are more densely packed in some areas at the beginning, see Fig. S2 in the supplementary material), we corrected for this by only displaying differences larger than the average distance between cells (7 μm).

Velocities

To calculate the velocities of cells, we used the distance the cells moved within a 30-minute interval (beginning at the start of the movie). The velocities of each cell were plotted at their positions at the beginning of the time interval using a banded LUT.

Trajectories of cell movements

To display the direction in which the cells moved we connected the two 2D coordinates of each cell at 30-minute intervals with a straight line. The colour of these lines represents the velocity of the cell (see Velocities).

Because of hemocytes, which patrol underneath the epithelium and thus block viewing of some of the histoblasts, 2% of histoblasts could not be followed all the way to the end of the movie (*n*=1296 cells). Thus, in some calculations that use two 2D coordinates, only the first coordinate could be determined. In these cases, the affected cells are coloured grey in the plots.

Three wild-type pupae (pupae #1, 2, 3) and one *en.Gal4 UAS.RedStinger* pupa (pupa #4) were used for these analyses. In total, 747 sister pairs were analysed. Pupa #4 differed from the other three only with respect to an increased number of cell deaths in the P compartment. To allow a classification of cells as either A or P compartment in the three wild-type pupae, the information from six *en.G4 UAS.RedStinger* movies was used.

Statistics

Since only angular data from 0° to 180° were considered, we used linear statistics. Data were tested for normal distribution using the Kolmogorov-Smirnov test. If the test excluded normal distribution, non-parametrical Mann-Whitney tests were performed. Analyses were performed using SPSS 16.0.

RESULTS

Histoblasts migrate to their final positions in two phases

Using 4D microscopy (Schnabel et al., 1997), we tracked the movements and divisions of the histoblasts while they spread more than 300 μm in 24 hours (Fig. 1A,B; see Movie 1 in the supplementary material). We tracked the cells at the tip of the moving cell mass, documented their positions, monitored their divisions, traced their descendants and studied their cell rearrangements. We can distinguish and follow all the cells of the A and P compartments (Fig. 1C,D; see Movie 2 in the supplementary material).

The histoblasts moved with an average speed of 15 μm/hour. Their maximum velocity of 46 μm/hour resembles that of fibroblasts extending their leading edge in tissue culture [42 μm/h (Abercrombie et al., 1970)].

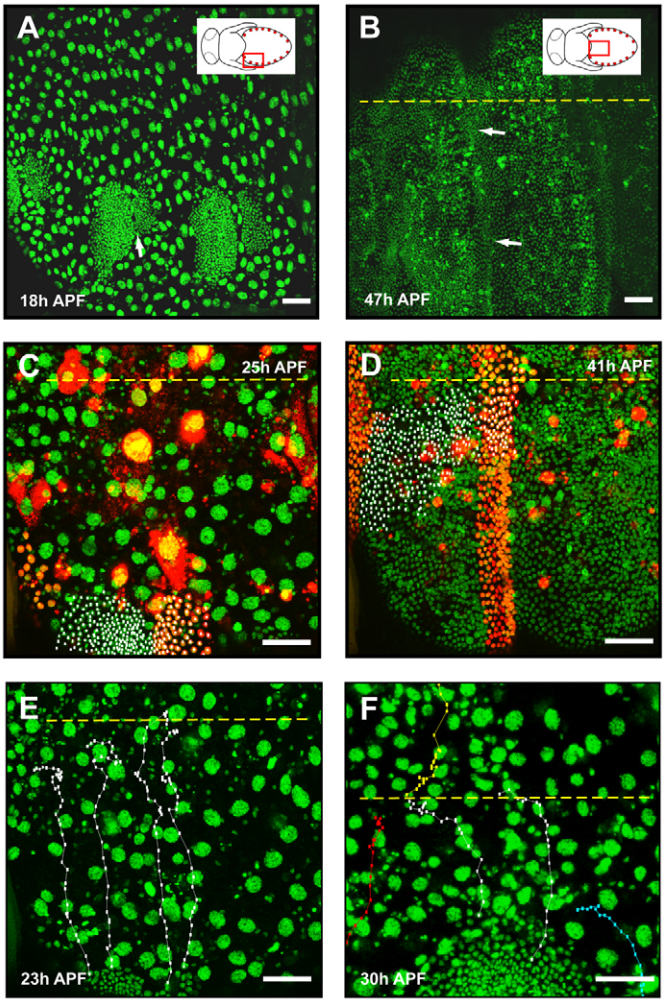

Fig. 1. 4D microscopy of histoblast migration during abdominal epidermis formation in *Drosophila*. (**A**,**B**) Development of dorsal histoblast nests. Dorsolateral view of segments 2 and 3. Nuclei of larval cells (large) and histoblasts (small) are visualised by Histone::GFP (green). Insets illustrate the location of the region shown. (A) At 18 hours after puparium formation (APF), the anterior and posterior dorsal histoblast nests fuse shortly before histoblast migration begins (arrow). (B) At 47 hours APF, the histoblasts have met at the dorsal midline and the whole abdomen is covered with adult cells. The segmental fold develops (arrows). See also Movie 1 in the supplementary material. (**C**,**D**) Tracking cells in a pupa in which the P compartment cells are marked with *en.Gal4* driving DsRed (pupa #4, segment 2). White dots indicate cells that were tracked using SIMI Biocell. See also Movie 2 in the supplementary material. (**E**,**F**) Representative paths of cells. (E) Cells move in a more or less straight line towards the dorsal midline. Some small detours are visible (pupa #4). (F) Cells of segment 2 (white) and 3 (blue) turn anteriorly when they approach the midline. Cells of segment 1 (red) do not turn. The most anterior cell of the opposite hemisegment (yellow) is positioned next to the most anterior cell of this hemisegment, illustrating the matching of cells of the two hemisegments at the midline (pupa #1). To achieve this registration, the white cell, which is positioned more posteriorly during its dorsal migration, moves further in an anterior direction than the yellow cell. In all images, anterior is to the left. Yellow dashed lines indicate the dorsal midline. Scale bars: 50 μm.

The histoblasts moved in two distinct phases. First, they followed a more or less straight line dorsally towards the midline for ~17 hours, starting at ~20 hours after puparium formation (APF) (Fig. 1E). Second, shortly before they reached the midline (at 37 hours APF), when there were about three rows of surviving LECs, the histoblasts turned in an anterior direction (Fig. 1F).

The histoblasts undergo about eight divisions (Madhavan and Madhavan, 1980), of which about two to four divisions occur during dorsal migration. During their spreading, the size of the histoblasts remains constant throughout the divisions (Ninov et al., 2007).

During the first, dorsal migration phase, the cells rearrange depending on their position along the anteroposterior axis

During dorsal migration, the histoblasts changed their arrangement relative to each other: the further posterior a cell was positioned, the further dorsal it moved (Fig. 2A; see Movies 3A,B in the supplementary material). This is because cells located more posteriorly moved dorsally towards the midline at a higher speed than those located more anteriorly (Fig. 2B; see Movie 4 in the supplementary material); they also moved for longer and made their anterior turn later (Fig. 2C).

The second, anterior migration phase completes the formation of the epithelium

As the histoblasts approached the midline, they slowed and turned to the anterior, now moving at about half their former speed (Fig. 3A). In some pupae, this change coincided with the disappearance of the last row of LECs – that which separates the histoblasts of neighbouring segments (see box in Fig. 3A). In this row, the LECs disappeared consecutively, so that the histoblasts came together like a zipper along the dorsoventral (DV) axis of the pupa (see earlier phases of spreading in Movie 1 in the supplementary material). In other pupae, this row of LECs disappeared earlier, at the time when there were still seven to nine rows of LECs separating the histoblasts from the midline (see Movies 1, 2 in the supplementary material). In this case, the histoblasts turned anteriorly later and only after they had reached the midline.

While moving anteriorly, the histoblasts started to disperse evenly (see Fig. S2 in the supplementary material) and adopted a more uniform shape, being elongated along the DV axis (Fig. 3B; see Movie 5 in the supplementary material). Histoblasts also stopped dividing and ceased to move relative to each other. Eventually, the intersegmental folds formed (see Movie 5 in the supplementary material) as the cells of the P compartment became folded underneath the A compartment, which further contributed to an anterior movement of the histoblasts. Thus, the dispersion of cells into the available space as they form a stable epithelium is directed anteriorly. This packing of cells resembles morphogenesis of the wing imaginal disc, where cells also become more uniformly packed shortly before hair formation (Classen et al., 2005). Only histoblasts of segments posterior to segment 1 migrated anteriorly, so that all the cells push up against the more stationary segment 1 (Fig. 1F; see Fig. S3 in the supplementary material).

Interestingly, the anterior movements of the histoblasts help match cells on either side of the midline. During the dorsal migration, the cells of the two facing hemisegments (left and right) do not head precisely towards each other but, as they turn anteriorly, they migrate to different extents so as to settle in precise registration across the midline (Fig. 1F). A similar matching of cells occurs during dorsal closure in *Drosophila* embryos (Millard and Martin, 2008).

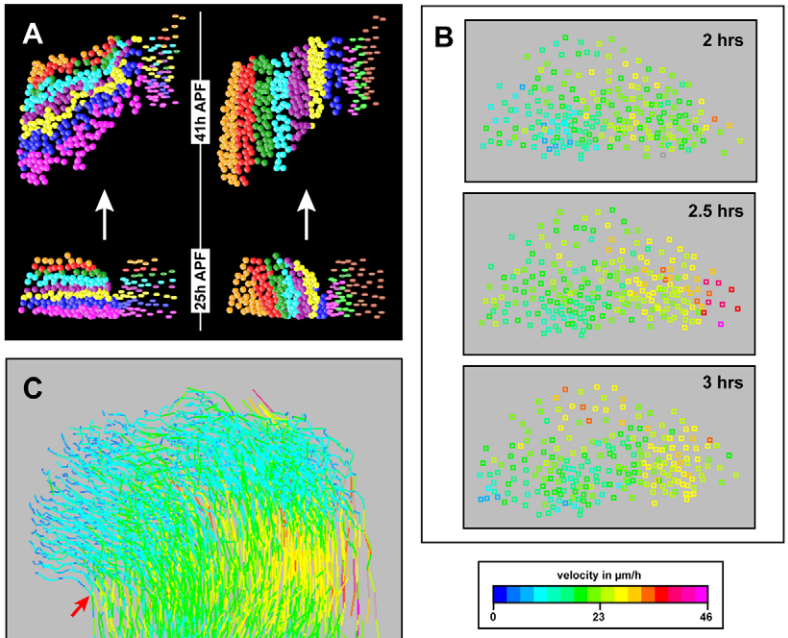

Fig. 2. The velocity and duration of the dorsal migration of cells determine their position. (**A**) Topology of the cell mass. The left and right panels show the same 3D representations of pupa #4 differently colour-coded to illustrate the change in cell positioning from 25 to 41 hours APF (*n*=273 and 443 cells, respectively). Spheres indicate anterior (A) compartment cells, and ovals indicate posterior (P) compartment cells. At the left, the cells are colour-coded arbitrarily in stripes with respect to the DV axis at the beginning of the recording; at the right, colour-coding is with respect to the AP axis at the end of the recording. The more posteriorly that cells are positioned the more dorsally they will move. Furthermore, cells do not change their positions along the AP axis. Cells in the P compartment appear to rearrange more extensively than those in A. Cells close to the A/P boundary move the furthest. See also Movies 3A,B in the supplementary material. (**B**) The velocity of each cell is plotted at its position at three consecutive time points (pupa #1). The number of hours after the start of the recording is indicated in the top right corner. The velocities of the cells change over time. Histoblasts which are more posterior in the segment tend to move faster. Cells are coloured grey if their velocity cannot be calculated because one of the coordinate-pair is missing. See also Movie 4 in the supplementary material. (**C**) The trajectories of all cells are plotted by connecting the coordinates of a cell in 30-minute intervals with a line (pupa #1). The colour of the line represents the velocity of the cells. More anteriorly positioned cells turn anteriorly earlier. The cell that turns first is marked with an arrow. More posteriorly positioned cells tend to move faster and turn anteriorly later. In all images, anterior is to the left.

Overall changes in neighbourhood relations are relatively small

Next, we analysed the behaviour of individual cells in the moving cell mass, particularly the dorsal migration, which is accompanied by cell divisions.

We first asked to what extent cells change their neighbours during their movements and found that most cells maintain their nearest neighbours (Fig. 4A); for example, only ~7% of sister cells lose contact with each other during their migration (Fig. 4B). Such stability of neighbour relations during morphogenesis is found in other developing epithelia, such as the pupal wing imaginal disc (Classen et al., 2005; Gibson et al., 2006). Even in the extending germband of the *Drosophila* embryo, where cells intercalate, the changes in neighbourhood relations are moderate (Bertet et al., 2004; Blankenship et al., 2006; Irvine and Wieschaus, 1994). Any changes in the relative positions of cells involve dynamic remodelling of cell-cell junctions (Bertet et al., 2004) (see Movies 5-7 in the supplementary material).

Changes in neighbourhood relations are most extensive at the A/P boundary

In certain regions, we observed histoblasts changing their neighbours. Those changes took place in the centre of the moving cell mass and especially near the boundary between the A and P compartments (Fig. 4A). In the centre of the cell mass, cells are more columnar and more densely packed and thus appeared to influence each other more strongly, which could lead to the separation of cells by the division or movement of neighbours that push in between them (Fig. 4C; see Movie 8 in the supplementary material). In most cases, this separated cells by no more than one cell diameter.

Those cells situated near the A/P boundary differed in their behaviour from other cells in the segment in that they moved furthest dorsally before they turned anteriorly (Fig. 2A; see Movies 3A,B in the supplementary material). Furthermore, they changed their neighbours more often (Fig. 4A); some sister cells even became separated by several cell diameters (see Movie 9 in the supplementary material). This unusual behaviour near the A/P border might be due to the unusual adhesive properties of the A/P boundary; it has been shown that cells of the two compartments do not mix because of the action of *engrailed* in the P compartment (Morata and Lawrence, 1975). Thus, the A/P boundary might be a region where cells are able to move more freely against each other, as there they adhere to each other less tightly.

The divisions of histoblasts are not oriented

Calculating the division angles relative to the direction of movement of the cell mass showed that the histoblast divisions are not preferentially oriented (Fig. 5A,B; see Table S1 in the supplementary material). Furthermore, divisions deviated from the direction of movement equally in the anterior and posterior directions. Indeed, there was no part of the moving cell mass where the orientation of cell division differed noticeably from the random (see Fig. S4 and Table S1 in the supplementary material) and thus it is the pattern of migrations that mostly shapes the adult segment.

In contrast to the abdomen, in both wing imaginal discs and the extending germband of *Drosophila*, oriented mitoses have been reported to contribute to morphogenesis (Baena-Lopez et al., 2005; da Silva and Vincent, 2007). This is perhaps because there it is the displacement of cells by mitoses and not cell rearrangements that affect the shape of the developing organ (Gibson et al., 2006).

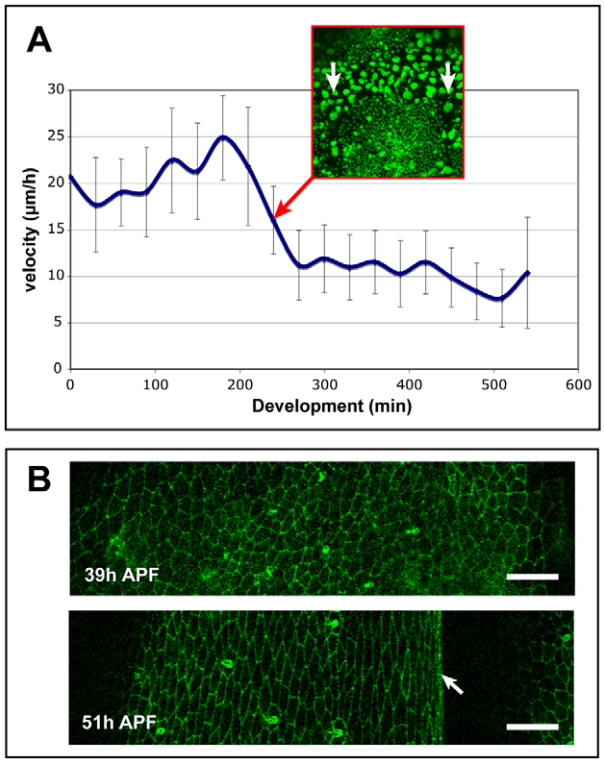

Fig. 3. The anterior migration of histoblasts. (**A**) The average velocity of all cells in 30-minute time intervals (pupa #1). Error bars show s.d. The red arrow indicates the time point when the first, most anteriorly positioned cells start to move anteriorly (see also arrow in Fig. 2C). About this time, the histoblasts slow down. The box shows the moving cell mass at this time point; one row of larval epithelial cells (LECs) still separates the histoblasts of neighbouring segments (white arrows). (**B**) The whole of segment 2 laterally of the midline. DE-cadherin::GFP marks the cell membranes. The upper panel shows the cell mass, which is moving in a DV direction, shortly before the histoblasts meet at the midline. The lower panel shows the same region 12 hours later, well after the cells have started to move anteriorly. Cells are much more organised now and tend to be uniformly shaped and elongated in the DV axis. The segmental groove can be seen (arrow). See also Movie 5 in the supplementary material. In all images, anterior is to the left. Scale bars: 25 µm.

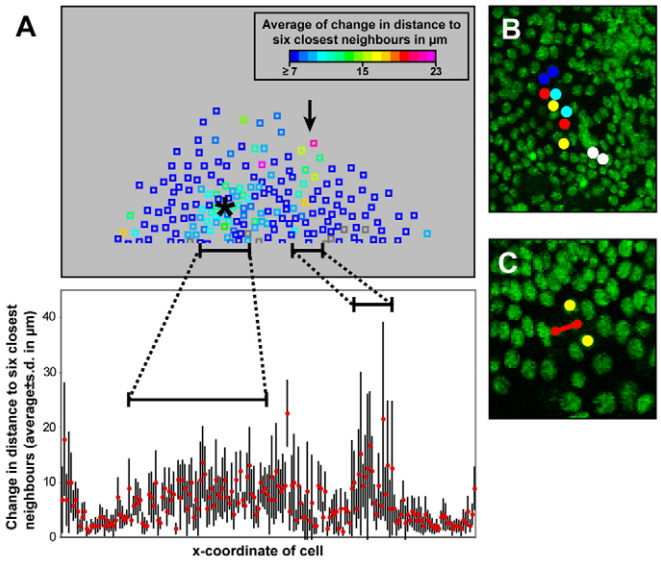

Fig. 4. Changes in neighbourhood relations between histoblasts. (**A**) (Top) Neighbourhood map. To calculate the neighbourhood map, the distances to the six closest neighbours at 30 hours APF were calculated for each cell. Then, the distances to the same six cells were calculated at 40 hours APF. For each of the six neighbours, the difference between these two values was calculated and then the average was plotted at the position of the cell at 30 hours APF (pupa #1). This value is a measure of changes in neighbourhood relations. Cells that were present at 30 hours APF but disappeared before 40 hours APF are coloured in grey. (Bottom) The averages shown in the neighbourhood map are plotted against the *x*-coordinates of the cells (error bars indicate s.d.). Black bars indicate the same regions in neighbourhood map and graph. The bars differ in size because at the bottom the coordinates are spread out along the *x*-axis. Most changes occur close to the A/P boundary (arrow) and in the centre of the cell mass, where cells are densest (asterisk). Some of the changes in the centre might be due to the spreading out of the cells, which is more extensive here because cells are very close together at the beginning (see Fig. S2 in the supplementary material). (**B**) Sister cells sometimes lose contact. Different sister cell pairs are colour-coded: blue, light blue and white remain neighbours, whereas red and yellow lose contact. (**C**) The division of a neighbouring cell (red line) separates sister cells (yellow).

Sister cells change their positions relative to each other in the direction of movement

After cell division, the two daughter cells change their position relative to each other. We measured the angle between the line connecting the two sisters and the DV axis, either at the last time point before their next division or at the end of the recording if there was no further division (Fig. 5A,C). We found that sister pairs became preferentially aligned with the DV rather than the anteroposterior (AP) axis (Fig. 5B; see Table S1 in the supplementary material). P compartment cells rearranged more extensively than A compartment cells (see Table S1 and Movies 3A,B in the supplementary material; see also Fig. 2A).

We then asked whether the rearrangement of sister cells is correlated with the direction of division of their mother. We found that sisters arising from divisions more or less along the DV axis were likely to remain in this orientation (Fig. 5D). More than 50% of sisters arising from divisions more or less orthogonal to the DV axis rearranged (Fig. 5D). The more the division of the mother cell deviated from the DV axis, the less likely was a rearrangement of the sister cells (Fig. 5E), suggesting that the rearrangement might not be an active process but largely due to the movement of the cell mass per se. This is supported by the observation that sister pairs in the P compartment, where cells move faster and for a longer period of time (Fig. 2B,C), rearranged more extensively (see Table S1 in the supplementary material).

Most sisters rearranged within the first 24 minutes after division (Fig. 5D), perhaps because rearrangement occurs when cell-cell contacts are still weak following mitosis.

The histoblasts appear to contribute actively to their own movement

In summary, we find that the morphogenesis of the abdominal epithelium is dominated by extensive cell movements that replace the LECs and deliver the histoblasts to their final positions. What drives these movements? One possibility is that the histoblasts actively contribute to their own displacement and move towards the

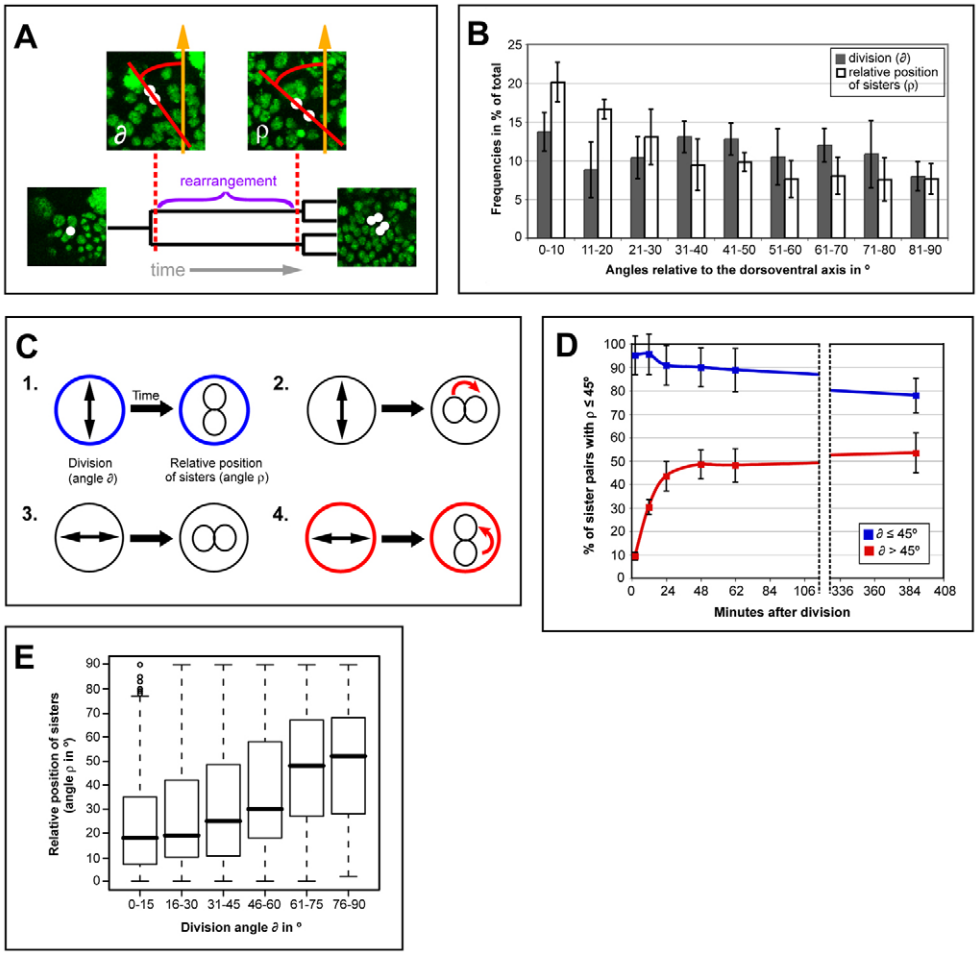

Fig. 5. Cell division orientation and change in position of sister cells relative to each other. (**A**) Determination of division orientation and the position of sister cells relative to each other (ρ). One frame after division, the angle relative to the DV axis was calculated (division angle ∂). Shortly before the first division of the sisters (or the end of the movie), the angle defining the position of the two sister cells relative to each other along the DV axis was calculated (ρ). In between division and the end of their cell cycle, the sister cells might rearrange relative to each other. (**B**) Bar chart showing the orientation of cell divisions (∂) and the position of sister cells (ρ) relative to the DV axis. Angles are shown on a 0° to 90° scale. The average angles are ∂=43±26° and ρ=36±26° (*n*=747 sister pairs). The groups differ significantly (see Table S1 in the supplementary material). After rearrangement, more sister pairs are oriented in the direction of movement (0°) than after mitosis. (**C**) Diagram illustrating possible outcomes of the rearrangement of sister cells after cell division. (1) Sisters do not change their relative position after a division along the DV axis (direction of movement). (2) Sisters rearrange themselves (red arrow) orthogonal to the DV axis after a division along the DV axis. (3) Sisters do not change their relative position after a division orthogonal to the DV axis. (4) Sisters rearrange themselves along the DV axis after a division orthogonal to the DV axis. Blue and red circles indicate the groups analysed in D. (**D**) Sister pairs that arose from divisions along the DV axis and retained this arrangement (blue) and sister pairs that arose from divisions orthogonal to the DV axis but rearranged along the DV axis (red). Most sisters whose mother divided in the direction of movement retained this arrangement, whereas ~50% of the sister cells whose mother divided orthogonally to the direction of movement rearrange. Most of these rearrangements occur within the first 24 minutes after division (*n*=747 sister pairs). (**E**) Analysis of the relationship of division orientation (∂) and the position of sister cells relative to each other (ρ). The division angles (in groups of 15°) are plotted against the corresponding angles representing the position of sisters relative to each other, shown as box plots (*n*=747 sister pairs). The medians indicate that ∂ correlates with ρ, which suggests that sisters are more likely to be arranged along the DV axis when the division of their mother had already biased their positioning. In all images, anterior is to the left and dorsal up. Error bars show s.d.

disappearing LECs. As the histoblasts approached the midline, we occasionally observed that the LECs retreated more slowly, and the histoblasts slowed down and started ‘whirling’ (Fig. 6A; see Movie 11 in the supplementary material), suggesting that the histoblasts ‘ran into’ the LECs. When the larval cells eventually disappeared, the histoblasts showed a surge of movement. These observations suggested to us that the histoblasts might move actively towards the LECs, pushing against them if they had not retreated in time. Furthermore, in many pupae, we observed a fold in the epithelial sheet, a few cell rows behind the most dorsal row of histoblasts, which developed as the histoblasts approached the midline (Fig. 6B). This could also be a consequence of a pushing force exerted by the histoblasts. This force could be generated by the extensive divisions in the centre of the moving cell mass and/or by the active crawling of the cells. The previously observed active planar intercalation of the histoblasts into the larval epithelium (Ninov et al., 2007) also supports the idea that the histoblasts actively contribute to the forces that drive the process.

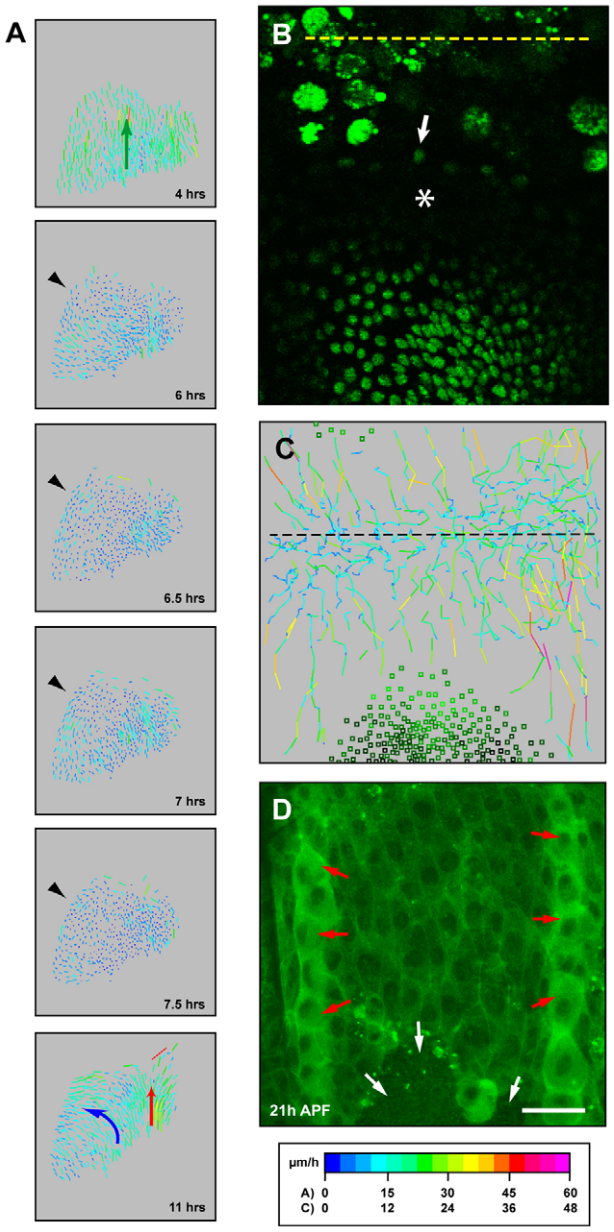

Fig. 6. Movement of histoblasts and LECs. (**A**) Six consecutive frames of Movie 11 (see Movie 11 in the supplementary material), which show the trajectories of all cells colour-coded according to their velocity (pupa #4). Cells move straight towards the midline (green arrow). Approaching the midline, they are hampered by the slowly retreating LECs, whereupon they slow down and undergo a whirling movement (arrowheads). Once the LECs have retreated, the cells suddenly move quickly anteriorly (blue arrow) and, in more posterior areas, towards the midline (red arrow). (**B**) The epithelial sheet is often folded (asterisk) near the last row of histoblasts touching the LECs (arrow). A yellow dashed line indicates the dorsal midline. (**C**) Trajectories of the dying and disappearing LECs illustrated by the same method as used in Fig. 2C (pupa #1). The approaching histoblasts are outlined with green squares. The LECs retreat more or less straight towards the midline. In the posterior part of the segment, they move slightly faster. At the midline, they tend to move anteriorly. The black dashed line indicates the dorsal midline. See also Movie 10 in the supplementary material. (**D**) Left hemisegment of segment 2 of a pupa expressing Sqh::GFP. White arrows indicate histoblasts. The LECs close to the segment borders (red arrows) express a higher level of Sqh::GFP than other LECs. In all images, anterior is to the left. Scale bar: 50 µm.

However, the observation that the histoblasts are hampered in their movement in those cases in which the LECs do not retreat in time, argues that the progression of histoblasts and the retreat of larval cells work together. Indeed, both the death of LECs and the division of histoblasts have been shown to be necessary for proper development (Ninov et al., 2007).

It might thus be possible that the dying larval cells also contribute to the movement of the histoblasts by pulling the moving cell mass forward as they constrict apically. Such 'apoptotic forces' have been suggested for the amnioserosa cells in dorsal closure (Toyama et al., 2008). We therefore studied how LECs disappear from the epithelium. Most dying LECs make contact with the histoblasts, but LECs that do not touch the histoblasts also die (Ninov et al., 2007): 18% of the LECs that disappear are located more than one larval cell diameter away from the histoblasts. Many LECs were observed to drift far dorsally, moving together with the histoblasts, before they were extruded from the epithelium (Fig. 6C; see Movies 10, 1 and 5 in the supplementary material). The LECs changed shape dynamically before they constricted apically (see Movie 5 in the supplementary material). Whether these dynamic movements and cell shape changes are able to generate a coordinated pulling force remains unclear.

Some LECs appear to canalise the dorsal migration of the histoblasts

The segmental groups of dorsally migrating histoblasts are typically separated by a row of LECs that persists almost until the histoblasts meet at the midline (Madhavan and Madhavan, 1980) (see box in Fig. 3A). These LECs, which lie at the future segment boundary, exhibited higher expression of Spaghetti squash (Sqh, Myosin II regulatory light chain) than the other larval cells (Fig. 6D). Similar cells expressing higher levels of Sqh have been found at the DV compartment boundary of wing discs and are thought to act as a fence between dorsal and ventral cells (Major and Irvine, 2006). The LECs at the segmental borders in the abdomen might also act as a fence, canalising the moving cell mass and restraining its lateral expansion. This behaviour would constitute one aspect of how the larval segmental 'blueprint' prefigures the adult pattern (Madhavan and Madhavan, 1980).

Histoblasts are removed by apoptosis

During the migration, 3% of the histoblasts disappeared (n=923); sometimes we observed the nucleus fragmenting (see Movie 12 in the supplementary material) and the cells constricting apically (see Movie 13 in the supplementary material). Hemocytes could be seen patrolling underneath these cells. Thus, it seems that histoblasts undergo apoptosis, as do the LECs (Ninov et al., 2007); for a morphological definition of apoptosis, see Galluzzi et al. (Galluzzi et al., 2007).

P compartment cells were much more likely to die than cells of the A compartment (10% in P versus 1% in A). Furthermore, most of the cell death (81%) occurred at the end of the dorsal migration, close to the midline or close to the segment boundaries. A possible explanation for this is that there is increased remodelling of cell-cell contacts at these regions owing to rearrangements of cells and/or the meeting of histoblasts of neighbouring segments. This might lead to more imbalances in the junctional network, which has been suggested as a reason for cell elimination (Farhadifar et al., 2007). Another possibility for the observed cell death is that the removed cells are less 'fit' than the remaining cells (Abrams, 2002).

DISCUSSION

We find that the formation of the abdominal epidermis differs from that of other epithelia, such as in the wing imaginal disc (Classen et al., 2005; Gibson et al., 2006) and during germband extension in the *Drosophila* embryo (Blankenship et al., 2006; Irvine and Wieschaus, 1994). In contrast to these more static epithelia, the formation of the abdominal epidermis is driven by extensive cell migrations. The final positioning of cells appears not to depend on the orientation of cell divisions, but particularly on cell movements, the speed and extent of which vary with the position along the AP axis (Fig. 2A-C). These movements also appear to lead to a rearrangement of sister cells in the direction of movement (Fig. 5B). During migration, cells only occasionally change their neighbours; the most extensive changes occur near the A/P boundary (Fig. 4A). These results explain why fluorescently marked wild-type clones tend to be elongated within the DV axis and do not split (see Fig. S5 in the supplementary material).

One explanation for the differential movements of cells within the AP axis could be a gradient of cell affinities (Lawrence et al., 1999). This gradient might be manifest in a differential stickiness of cells along the AP axis, with posterior cells adhering less to each other, allowing their more extensive rearrangement (see Fig. S6 in the supplementary material).

Interestingly, the behaviour of the cells in the moving epithelial sheet appears to be influenced by the presence of the A/P boundary (see Fig. S6 in the supplementary material). The A/P boundary, with its differential adhesive properties, seems to act like an expansion joint, allowing cells to move more freely along each other (see Movie 9 in the supplementary material). Thus, the A/P boundary is not only important for the patterning of the A and P compartments (Zecca et al., 1995), but also appears to influence the positioning of the histoblasts.

In addition, we find that the A and the P compartment cells behave differently, with cells of the P compartment rearranging more extensively (Fig. 2A; see Table S1 in the supplementary material) and also being more likely to undergo cell death. These findings highlight the differences between the A and P compartments, which may act as two independent fields (Crick and Lawrence, 1975), and provide insights into differences in cellular behaviours.

In many developmental contexts, cells need to coordinate their behaviour; for example, in order to move as a group (Lecaudey and Gilmour, 2006). Our work complements the study of Ninov et al. (Ninov et al., 2007), who focussed their analysis on the interactions of histoblasts and LECs, and highlights the behaviour of individual cells, the sum of which is responsible for morphogenesis. A combination of cell tracking using 4D microscopy and clonal analysis should help us tackle questions such as what mechanisms guide the cells to their final position and what positions them relative to each other. Addressing these questions is important in order to understand the morphogenesis of all epithelia, including in gastrulation and neurulation (Keller, 2002).

Acknowledgements

We thank Kyra Campbell, Luis M. Escudero, Rita Sinka, Jean-Paul Vincent and the Bloomington Stock Centre for flies; Steve Ellis for building the incubation chamber; Caroline Fabre for flies and helpful discussions; Verena Dietrich-Bischoff for critically reading the manuscript and helpful discussions; José Casal for flies, advice, critically reading the manuscript and helpful discussions; Peter A. Lawrence for advice, critically reading the manuscript, helpful discussions and help in writing the manuscript. This work was supported by the Wellcome Trust grant 079204/Z/06/Z (Z.C.), the Medical Research Council (M.B.), a DFG research fellowship (M.B.) and the Wellcome Trust grant WD078889MA to Peter A. Lawrence in whose laboratory the work was conducted. Deposited in PMC for release after 6 months.

Author contributions

M.B. planned and performed the experiments and wrote the manuscript. Z.C. wrote the software to analyse the SIMI Biocell data and commented on the manuscript.

Supplementary material

Supplementary material for this article is available at http://dev.biologists.org/cgi/content/full/136/14/2403/DC1

References

Abercrombie, M., Heaysman, J. E. and Pegrum, S. M. (1970). The locomotion of fibroblasts in culture. I. Movements of the leading edge. *Exp. Cell Res.* **59**, 393-398.

Abrams, J. M. (2002). Competition and compensation: coupled to death in development and cancer. *Cell* **110**, 403-406.

Baena-Lopez, L. A., Baonza, A. and Garcia-Bellido, A. (2005). The orientation of cell divisions determines the shape of *Drosophila* organs. *Curr. Biol.* **15**, 1640-1644.

Bainbridge, S. P. and Bownes, M. (1981). Staging the metamorphosis of *Drosophila* melanogaster. *J. Embryol. Exp. Morphol.* **66**, 57-80.

Bertet, C., Sulak, L. and Lecuit, T. (2004). Myosin-dependent junction remodelling controls planar cell intercalation and axis elongation. *Nature* **429**, 667-671.

Blankenship, J. T., Backovic, S. T., Sanny, J. S., Weitz, O. and Zallen, J. A. (2006). Multicellular rosette formation links planar cell polarity to tissue morphogenesis. *Dev. Cell* **11**, 459-470.

Chen, Y. and Zhao, X. (1998). Shaping limbs by apoptosis. *J. Exp. Zool.* **282**, 691-702.

Clarkson, M. and Saint, R. (1999). A His2AvDGFP fusion gene complements a lethal His2AvD mutant allele and provides an in vivo marker for *Drosophila* chromosome behavior. *DNA Cell Biol.* **18**, 457-462.

Classen, A. K., Anderson, K. I., Marois, E. and Eaton, S. (2005). Hexagonal packing of *Drosophila* wing epithelial cells by the planar cell polarity pathway. *Dev. Cell* **9**, 805-817.

Crick, F. H. and Lawrence, P. A. (1975). Compartments and polyclones in insect development. *Science* **189**, 340-347.

da Silva, S. M. and Vincent, J. P. (2007). Oriented cell divisions in the extending germband of *Drosophila*. *Development* **134**, 3049-3054.

Escudero, L. M., Bischoff, M. and Freeman, M. (2007). Myosin II regulates complex cellular arrangement and epithelial architecture in *Drosophila*. *Dev. Cell* **13**, 717-729.

Farhadifar, R., Roper, J. C., Aigouy, B., Eaton, S. and Julicher, F. (2007). The influence of cell mechanics, cell-cell interactions, and proliferation on epithelial packing. *Curr. Biol.* **17**, 2095-2104.

Galluzzi, L., Maiuri, M. C., Vitale, I., Zischka, H., Castedo, M., Zitvogel, L. and Kroemer, G. (2007). Cell death modalities: classification and pathophysiological implications. *Cell Death Differ.* **14**, 1237-1243.

Gibson, M. C., Patel, A. B., Nagpal, R. and Perrimon, N. (2006). The emergence of geometric order in proliferating metazoan epithelia. *Nature* **442**, 1038-1041.

Gong, Y., Mo, C. and Fraser, S. E. (2004). Planar cell polarity signalling controls cell division orientation during zebrafish gastrulation. *Nature* **430**, 689-693.

Grumbling, G. and Strelets, V. (2006). FlyBase: anatomical data, images and queries. *Nucleic Acids Res.* **34**, D484-D488.

Irvine, K. D. and Wieschaus, E. (1994). Cell intercalation during *Drosophila* germband extension and its regulation by pair-rule segmentation genes. *Development* **120**, 827-841.

Jacinto, A., Wood, W., Balayo, T., Turmaine, M., Martinez-Arias, A. and Martin, P. (2000). Dynamic actin-based epithelial adhesion and cell matching during Drosophila dorsal closure. *Curr. Biol.* **10**, 1420-1426.

Keller, P. J., Schmidt, A. D., Wittbrodt, J. and Stelzer, E. H. (2008). Reconstruction of zebrafish early embryonic development by scanned light sheet microscopy. *Science* **322**, 1065-1069.

Keller, R. (2002). Shaping the vertebrate body plan by polarized embryonic cell movements. *Science* **298**, 1950-1954.

Lawrence, P. A., Casal, J. and Struhl, G. (1999). The hedgehog morphogen and gradients of cell affinity in the abdomen of *Drosophila*. *Development* **126**, 2441-2449.

Lecaudey, V. and Gilmour, D. (2006). Organizing moving groups during morphogenesis. *Curr. Opin. Cell Biol.* **18**, 102-107.

Madhavan, M. M. and Madhavan, K. (1980). Morphogenesis of the epidermis of adult abdomen of *Drosophila*. *J. Embryol. Exp. Morphol.* **60**, 1-31.

Major, R. J. and Irvine, K. D. (2006). Localization and requirement for Myosin II at the dorsal-ventral compartment boundary of the *Drosophila* wing. *Dev. Dyn.* **235**, 3051-3058.

Manjon, C., Sanchez-Herrero, E. and Suzanne, M. (2007). Sharp boundaries of Dpp signalling trigger local cell death required for *Drosophila* leg morphogenesis. *Nat. Cell Biol.* **9**, 57-63.

McMahon, A., Supatto, W., Fraser, S. E. and Stathopoulos, A. (2008). Dynamic analyses of *Drosophila* gastrulation provide insights into collective cell migration. *Science* **322**, 1546-1550.

Millard, T. H. and Martin, P. (2008). Dynamic analysis of filopodial interactions during the zippering phase of *Drosophila* dorsal closure. *Development* **135**, 621-626.
Morata, G. and Lawrence, P. A. (1975). Control of compartment development by the engrailed gene in *Drosophila*. *Nature* **255**, 614-617.
Ninov, N., Chiarelli, D. A. and Martin-Blanco, E. (2007). Extrinsic and intrinsic mechanisms directing epithelial cell sheet replacement during *Drosophila* metamorphosis. *Development* **134**, 367-379.
Oda, H. and Tsukita, S. (2001). Real-time imaging of cell-cell adherens junctions reveals that *Drosophila* mesoderm invagination begins with two phases of apical constriction of cells. *J. Cell Sci.* **114**, 493-501.
Roseland, C. R. and Schneiderman, H. A. (1979). Regulation and Metamorphosis of the abdominal histoblasts of *Drosophila melanogaster*. *Wilhelm Roux's Arch.* **186**, 235-265.
Royou, A., Sullivan, W. and Karess, R. (2002). Cortical recruitment of nonmuscle myosin II in early syncytial *Drosophila* embryos: its role in nuclear axial expansion and its regulation by Cdc2 activity. *J. Cell Biol.* **158**, 127-137.
Schnabel, R., Hutter, H., Moerman, D. G. and Schnabel, H. (1997). Assessing normal embryogenesis in *C. elegans* using a 4D-microscope: variability of development and regional specification. *Dev. Biol.* **184**, 234-265.
Schnabel, R., Bischoff, M., Hintze, A., Schulz, A. K., Hejnol, A., Meinhardt, H. and Hutter, H. (2006). Global cell sorting in the *C. elegans* embryo defines a new mechanism for pattern formation. *Dev. Biol.* **294**, 418-431.
Struhl, G. and Basler, K. (1993). Organizing activity of wingless protein in *Drosophila*. *Cell* **72**, 527-540.
Struhl, G., Barbash, D. A. and Lawrence, P. A. (1997). Hedgehog organises the pattern and polarity of epidermal cells in the *Drosophila* abdomen. *Development* **124**, 2143-2154.
Tawk, M., Araya, C., Lyons, D. A., Reugels, A. M., Girdler, G. C., Bayley, P. R., Hyde, D. R., Tada, M. and Clarke, J. D. (2007). A mirror-symmetric cell division that orchestrates neuroepithelial morphogenesis. *Nature* **446**, 797-800.
Toyama, Y., Peralta, X. G., Wells, A. R., Kiehart, D. P. and Edwards, G. S. (2008). Apoptotic force and tissue dynamics during *Drosophila* embryogenesis. *Science* **321**, 1683-1686.
Voiculescu, O., Bertocchini, F., Wolpert, L., Keller, R. E. and Stern, C. D. (2007). The amniote primitive streak is defined by epithelial cell intercalation before gastrulation. *Nature* **449**, 1049-1052.
Zecca, M., Basler, K. and Struhl, G. (1995). Sequential organizing activities of engrailed, hedgehog and decapentaplegic in the *Drosophila* wing. *Development* **121**, 2265-2278.